Acta Crystallographica Section F
Structural Biology and Crystallization Communications
ISSN 1744-3091

Crystallization and preliminary X-ray analysis of the complexes between a Fab and two forms of human insulin-like growth factor II

Janet Newman,[a]* Edward H. Cohen,[b] Leah Cosgrove,[a] Kris Kopacz,[b] Daniel T. Dransfield,[b] Timothy E. Adams[a] and Thomas S. Peat[a]

[a]Molecular and Health Technologies, CSIRO, 343 Royal Parade, Parkville, VIC 3052, Australia, and [b]Dyax Corp, 300 Technology Square, Cambridge, MA 02139, USA

Correspondence e-mail: janet.newman@csiro.au

Received 13 June 2009
Accepted 29 June 2009

Elevated expression of insulin-like growth factor II (IGF-II) is frequently observed in a variety of human malignancies, including breast, colon and liver cancer. As IGF-II can deliver a mitogenic signal through both the type 1 insulin-like growth factor receptor (IGF-IR) and an alternately spliced form of the insulin receptor (IR-A), neutralizing the biological activity of this growth factor directly is an attractive therapeutic option. One method of doing this would be to find antibodies that bind tightly and specifically to the peptide, which could be used as protein therapeutics to lower the peptide levels *in vivo* and/or to block the peptide from binding to the IGF-IR or IR-A. To address this, Fabs were selected from a phage-display library using a biotinylated precursor form of the growth factor known as IGF-IIE as a target. Fabs were isolated that were specific for the E-domain C-terminal extension and for mature IGF-II. Four Fabs selected from the library were produced, complexed with IGF-II and set up in crystallization trials. One of the Fab–IGF-II complexes (M64-F02–IGF-II) crystallized readily, yielding crystals that diffracted to 2.2 Å resolution and belonged to space group $P2_12_12_1$, with unit-cell parameters a = 50.7, b = 106.9, c = 110.7 Å. There was one molecule of the complete complex in the asymmetric unit. The same Fab was also crystallized with a longer form of the growth factor, IGF-IIE. This complex crystallized in space group $P2_12_12_1$, with unit-cell parameters a = 50.7, b = 107, c = 111.5 Å, and also diffracted X-rays to 2.2 Å resolution.

1. Introduction

IGF-II is a maternally imprinted growth factor that plays a key role in promoting embryonic growth. Genetic inactivation of the active paternally inherited *Igf-II* allele results in foetal growth retardation in mice (DeChiara *et al.*, 1990); in contrast, co-expression of both alleles is associated with somatic overgrowth of mouse embryos (Leighton *et al.*, 1995). At the cellular level, IGF-II and the related growth factor IGF-I bind to and activate IGF-IR, a heterotetrameric transmembrane tyrosine kinase that is expressed in many tissues, eliciting a spectrum of biological responses including proliferation, migration and protection from programmed cell death (apoptosis; Adams *et al.*, 2000). In addition, IGF-II binds with high affinity to IR-A, which is preferentially expressed in foetal tissues (Frasca *et al.*, 1999). Activation of IR-A by insulin results in a largely metabolic response at the cellular level, whereas activation by IGF-II primarily delivers a mitogenic effect (Frasca *et al.*, 1999).

The biosynthesis of human IGF-II is accompanied by complex post-translational modifications (Khosla *et al.*, 2002). The primary translation product comprises a signal peptide (24 amino acids)

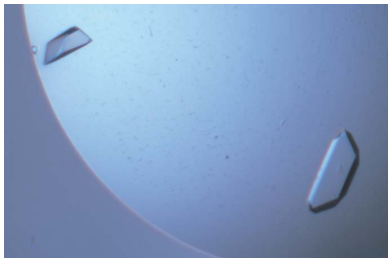

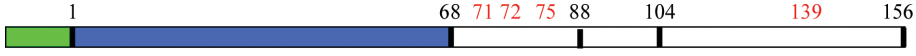

Figure 1
A cartoon showing the make-up of the human IGF-II peptide, showing the sites of glycosylation and the possible cleavage sites. The signal peptide (24 residues) is shown in green and the mature IGF-II (residues 1–67; domains B, C, A, D) is shown in blue. Glycosylation sites are labelled with red numbers and cleavage sites with black numbers.

followed by a 67-amino-acid sequence corresponding to the mature form of IGF-II (domains B, C, A and D) and a C-terminal extension of 89 amino acids designated the E domain (Fig. 1). Following the removal of the signal peptide, O-linked glycosylation and endoproteolysis give rise to multiple processing intermediates and isoforms (Duguay *et al.*, 1998) which may be present in normal serum (Valenzano *et al.*, 1995). Although expression of the growth factor is typically down-regulated in many tissues following birth, elevated expression of IGF-II is frequently observed in a variety of human malignancies, including liver and colorectal cancer (Jacobs, 2008; Breuhahn & Schirmacher, 2008). Aberrant processing and variable glycosylation resulting in the secretion of high-molecular-weight forms of IGF-II may also be observed (Hizuka *et al.*, 1998; Khosla *et al.*, 2002).

As IGF-II exerts its biological effects by binding to and activating both IGF-IR and IR-A, neutralizing the biological activity of this growth factor directly is an attractive therapeutic option. We have isolated Fabs from a human phage-display library antibody with high affinity for human IGF-II (Dransfield *et al.*, manuscript in preparation). We report the crystallization and preliminary X-ray analysis of one of these Fabs, M064-F02, in complex with both mature IGF-II and IGF-IIE.

2. Materials and methods

2.1. Production of Fabs

IGF-IIE (consisting of domains B, C, A, D and E) was biotinylated to aid downstream processing and was then used as a target for panning of a human Fab-displaying phage library (Hoet *et al.*, 2005). Four Fabs were selected which showed tight (subnanomolar) binding to the target IGF-IIE and all four of these also bound to IGF-II with subnanomolar affinity (Dransfield *et al.*, manuscript in preparation).

For each of four isolates obtained from the phage-display library, TG1 *Escherichia coli* cells containing a plasmid encoding the Fab fragment of the antibody gene of interest were grown overnight at 303 K in 2× NZCYM medium supplemented with 100 µg ml^{-1} ampicillin. The following day, the cultures were diluted 1:100 in fresh 2× NZCYM + ampicillin media and grown at 310 K until an OD_{600} of 0.8–1.0 was reached. The cultures were then induced with 1 m*M* IPTG and grown overnight at 303 K. Bacterial cultures were then pelleted and the supernatants were subjected to standard Protein A purification techniques. The purified Fabs were buffer-exchanged into 25 m*M* ammonium acetate, 100 m*M* sodium chloride and concentrated to 3.8–7.6 mg ml^{-1} depending on the specific Fab.

2.2. Crystallization and data collection

Human IGF-II (residues 1–67, 7469 Da) was purchased from Novozymes GroPep (Thebarton, South Australia) and was stored at a concentration of either 10 or 1 mg ml^{-1} in 10 m*M* HCl. The peptide was neutralized with sodium hydroxide before use. The complexes between IGF-II and the Fab molecules were formed by adding neutralized peptide to the Fab in a 2:1 peptide:Fab molar ratio; the complexes thus formed were used without further purification.

Initial sitting-drop vapour-diffusion crystallization trials were set up at the Bio21 Collaborative Crystallization Centre (Bio21 C3) in Innovaplate SD-2 crystallization plates (Innovadyne, California) using crystallization droplets of 200 nl total initial volume with a protein:crystallant ratio of 1:1 and a reservoir volume of 50 µl. Two 96-condition screens, the JCSG+ Suite and the PACT Suite (Qiagen Pty Ltd, Doncaster, Victoria; Newman *et al.*, 2005), were tested against the four Fab–IGF-II complexes. The plates were set up and incubated at 293 K. Crystals were observed in over 30 droplets for the M64-F02–IGF-II complex after 1 d. All the drops for the other complexes showed no signs of crystallizing even after two months. An optimization screen consisting of a random (that is, akin to CrysTools; Segelke & Rupp, 1998) combination of the factors common to the crystallization hits was created using the optimization tool in CrystalTrak (Rigaku Automation, Carlsbad, California) and this was used to set up further droplets. This optimization screen was set up in two vapour-diffusion experiments, one in which the reservoir solution was the crystallant itself, which we refer to as 'standard', and one in which 1.5 *M* sodium chloride was used in all reservoirs (Newman, 2005). All optimization experiments were performed in the same SD-2 plates as the initial screening. Many (>10) small crystals were observed in most of the droplets equilibrated against salt after 1 d. After a week, larger crystals were found in almost all droplets in the standard optimization plate. All the crystals used in the subsequent analyses were harvested from this standard optimization plate. A crystal grown in 118 m*M* calcium chloride, 18.5%(*w*/*v*) PEG 6000, 10%(*v*/*v*) PCB (propionate–cacodylate–bis-tris propane buffer; Newman, 2004) pH 5.3 (Fig. 2) was harvested and cryoprotected by adding 1 µl of a cryosolution containing 80%(*v*/*v*) reservoir solution, 10%(*v*/*v*) ethylene glycol and 10%(*v*/*v*) glycerol to the crystallization droplet and then immediately harvesting a crystal from the drop. The crystal was flash-cooled in the nitrogen-gas stream at beamline PX1

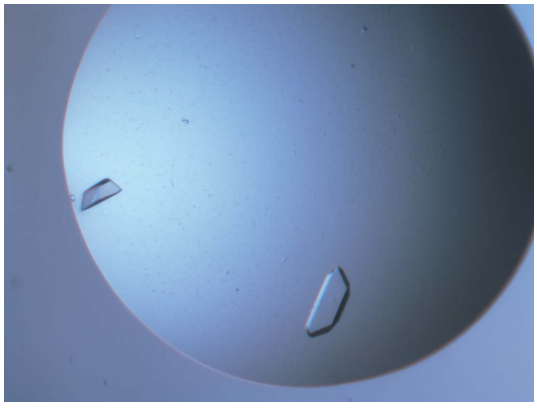

Figure 2
Crystals of the M64-F02–IGF-II complex. The large crystal is 22 µm in the longest dimension.

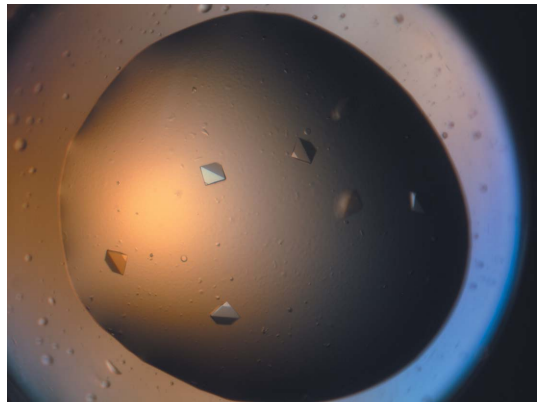

Figure 3
Crystals of the M64-F02–IGF-IIE complex. The crystals are approximately 130 µm measured diagonally across the crystals.

Table 1
Sample information for M64-F02–IGF-II.

Macromolecule details	
Component molecules	M64-F02 antibody, insulin-like growth factor II
Macromolecular assembly	M64-F02 antibody Fab complexed with IGFII
Mass (Da)	50 000 + 7469
Source organism	*Escherichia coli*
Macromolecule production	
M64-F02 antibody	
Target selection	The Fab was selected from a library using a biotinylated IGF-IIE target
Crystallization and crystal data	
Crystallization method	Sitting-drop vapour diffusion
Temperature (K)	293
Apparatus	Innovadyne SD2 plate
Atmosphere	1
Crystal-growth time (d)	2–3
Seeding	None
Additional details	
Crystallization solutions	
Macromolecule	0.2 µl 4 mg ml^{-1} M64-F02–IGF-II complex
Precipitant	0.1 µl 18.5%(*w*/*v*) polyethylene glycol 3350, 10%(*v*/*v*) propionate–cacodylate–bis-tris propane, 118 m*M* calcium chloride pH 5.31
Reservoir	50 µl 18.5%(*w*/*v*) polyethylene glycol 3350, 10%(*v*/*v*) propionate–cacodylate–bis-tris propane, 118 m*M* calcium chloride pH 5.31
Crystal data	
Crystal size (mm)	0.225 × 0.090 × 0.020
Matthews coefficient V_M (Å^3 Da^{-1})	2.60
Solvent content (%)	52.8
Unit-cell data	
Crystal system, space group	Orthorhombic, $P2_12_12_1$
a, *b*, *c* (Å)	50.67, 106.92, 110.66
α, β, γ (°)	90, 90, 90
No. of molecules in unit cell, *Z*	4

Table 2
Data-collection and structure-solution statistics for M64-F02–IGF-II.

Values in parentheses are for the outer shell.

Diffraction source	PX1, Australian Synchrotron
Wavelength (Å)	0.98
Detector	ADSC Quantum 210r
Temperature (K)	100
Resolution range (Å)	55–2.2
No. of unique reflections	27548
Completeness (%)	89.9 (90.0)
Redundancy	5.0 (5.0)
$\langle I/\sigma(I)\rangle$	6.3 (1.5)
R_{merge}†	9.5 (47.5)
Data-processing software	*MOSFLM*

† $R_{merge} = \sum_{hkl}\sum_i |I_i(hkl) - \langle I(hkl)\rangle| / \sum_{hkl}\sum_i I_i(hkl)$, where $I_i(hkl)$ is the intensity of an observation and $\langle I(hkl)\rangle$ is the mean value for its unique reflection; summations are over all reflections.

Table 3
Sample information for M64-F02–IGF-IIE.

Macromolecule details	
Component molecules	M64-F02 antibody, insulin-like growth factor II precursor
Macromolecular assembly	M64-F02 antibody Fab complexed with IGF-IIE
Mass (Da)	50 000 + 11 949
Source organism	*Escherichia coli*
Macromolecule production	
M64-F02 antibody	
Target selection	The Fab was selected from a library using a biotinylated IGF-IIE target
Crystallization and crystal data	
Crystallization method	Sitting-drop vapour diffusion
Temperature (K)	293
Apparatus	Innovadyne SD2 plate
Atmosphere	1
Crystal-growth time (d)	2–3
Seeding	None
Additional details	
Crystallization solutions	
Macromolecule	0.5 µl 4 mg ml^{-1} M64-F02–IGF-II complex
Precipitant	0.5 µl 17.4%(*w*/*v*) polyethylene glycol 3350, 256 m*M* ammonium formate
Reservoir	50 µl 17.4%(*w*/*v*) polyethylene glycol 3350, 256 m*M* ammonium formate
Crystal data	
Crystal size (mm)	0.100 × 0.100 × 0.050
Matthews coefficient V_M (Å^3 Da^{-1})	2.44
Solvent content (%)	49.5
Unit-cell data	
Crystal system, space group	Orthorhombic, $P2_12_12_1$
a, *b*, *c* (Å)	50.72, 106.95, 111.48
α, β, γ (°)	90, 90, 90
No. of molecules in unit cell, *Z*	4

Table 4
Data-collection and structure-solution statistics for M64-F02–IGF-IIE.

Values in parentheses are for the outer shell.

Diffraction source	PX1, Australian Synchrotron
Wavelength (Å)	0.98
Detector	ADSC Quantum 210r
Temperature (K)	100
Resolution range (Å)	77–2.2
No. of unique reflections	31608
Completeness (%)	99.9 (100)
Redundancy	7.2 (7.2)
$\langle I/\sigma(I)\rangle$	5.9 (1.2)
R_{merge}†	11.5 (62.3)
Data-processing software	MOSFLM

† $R_{merge} = \sum_{hkl}\sum_i |I_i(hkl) - \langle I(hkl)\rangle| / \sum_{hkl}\sum_i I_i(hkl)$, where $I_i(hkl)$ is the intensity of an observation and $\langle I(hkl)\rangle$ is the mean value for its unique reflection; summations are over all reflections.

of the Australian Synchrotron. 181 frames of 1° oscillations were collected, each frame being exposed for 8 s.

An IGF-IIE variant (residues 1–104, 11 949 Da) was purchased from Novozymes GroPep (Thebarton, South Australia) and was provided as a lyophilized powder. The complex was formed by adding M64-F02 Fab at 4 mg ml^{-1} directly to a vial containing the lyophilized IGF-IIE to give a molar ratio of 2:1 peptide:Fab and gently agitating to resuspend the solid peptide. The complex was used without further modification. This complex was set up in SD-2 plates with a reservoir volume of 50 µl at 293 K in droplets consisting of 100 nl complex with 100 nl reservoir using the JCSG+ Suite and the optimization screen based on the successful conditions for the M64-F02–IGF-II complex. This initial screening gave 11 hits from the JCSG+ Suite and four from the optimization screen. Of the 11 hits from the JCSG+ Suite, nine contained PEG 3350 and the other two contained PEG 6000 and PEG MME 2K, respectively. A new random optimization screen of 96 conditions was created based on these 15 hits and was used for another round of crystallization. In this case, droplets of 0.5 µl + 0.5 µl were used. Crystals appeared within a day in over 60 of the drops in this optimization screen (Fig. 3). 16 crystals from this plate were tested on beamline PX1 of the Australian Synchrotron; some were cryocooled in a nitrogen-gas stream, some were cryocooled by plunging into liquid nitrogen and some were cooled with and some without additional cryoprotection. Only one showed any significant diffraction and a data set was collected to 3 Å resolution from this crystal. The crystals were easily crushed during harvesting and tended to stick to the crystallization plate.

A PX Scanner (Varian, UK) was used to test the diffraction quality of 49 crystals *in situ* in this optimization plate (6 × 100 s or 10 min of X-ray exposure per crystal). Of the 49 crystals scanned, only 20 showed any diffraction and showed *in situ* diffraction extending beyond 4 Å resolution. A crystal from well E10 showed *in situ* diffraction extending to 3.3 Å resolution. This crystal was hardened by injecting 1 µl of a 1:10^4 dilution of 25% gluteraldehyde solution into the 50 µl reservoir 2 h prior to harvesting. The crystal was cryoprotected by adding 2 µl of a cryosolution [made up of the

reservoir but with 20%(*v*/*v*) of the water replaced with 10%(*v*/*v*) glycerol and 10%(*v*/*v*) ethylene glycol] to the droplet containing the crystal and immediately harvesting the crystal. The crystal was flash-cooled in the nitrogen-gas stream on beamline PX1 of the Australian Synchrotron and data extending to 2.2 Å resolution were collected.

3. Results and discussion

After performing the selection for binders against the biotinylated IGF-IIE target, four Fabs were selected for continued investigation: M63-F02, M64-E04, M64-F02 and M72-G06. The four Fabs were each concentrated to ∼5 mg ml^{-1} and complexed in a 1:2 molar ratio with IGF-II. One of these complexes crystallized and after one cycle of optimization a crystal of the M64-F02–IGF-II complex was harvested from a condition containing 118 m*M* calcium chloride, 10%(*v*/*v*) PCB buffer pH 5.31 and 18.5%(*w*/*v*) PEG 6000. X-ray data were collected from the cryogenically cooled crystal to 2.2 Å resolution on beamline PX1 of the Australian Synchrotron. The crystal was somewhat mosaic but the data were processed smoothly in *MOSFLM* (Leslie, 1992), yielding a data set which was 89.9% complete overall (Tables 1 and 2). Molecular replacement using the coordinates of the Fab from PDB entry 1igf (chains L and H) was attempted with the *Phenix* package (Adams *et al.*, 2004) and gave a solution with an initial *R* value of 47%. Both standard vapour-diffusion experiments and vapour-diffusion experiments against a 1.5 *M* sodium chloride reservoir were set up for this complex and although both gave crystals, it was a crystal from the standard vapour-diffusion experiment that was used to collect data. The sodium chloride reservoir plates produced more smaller crystals and these crystals grew overnight. This suggested that the sodium chloride reservoir solution was too concentrated for optimal crystal growth, although further experiments were not performed to test this.

The same Fab M64-F02 was complexed with IGF-IIE, a longer form of insulin-like growth factor. Crystals of a different morphology from the M64-F02–IGF-II complex grew under somewhat similar conditions. A crystal that grew from a reservoir solution containing 256 m*M* ammonium formate, 17.4%(*w*/*v*) PEG 3350 was lightly cross-linked, cryoprotected and flash-cooled in the stream. Data were collected to 2.2 Å resolution on beamline PX1 of the Australian Synchrotron. Molecular replacement using the M64-F02–IGF-II coordinates gave an unambiguous solution (Tables 3 and 4).

Cycles of refinement and model building are proceeding on both complexes.

We thank the Bio21 Collaborative Crystallization Centre and the Australian Synchrotron.

References

Adams, P. D., Gopal, K., Grosse-Kunstleve, R. W., Hung, L.-W., Ioerger, T. R., McCoy, A. J., Moriarty, N. W., Pai, R. K., Read, R. J., Romo, T. D., Sacchettini, J. C., Sauter, N. K., Storoni, L. C. & Terwilliger, T. C. (2004). *J. Synchrotron Rad.* **11**, 53–55.
Adams, T. E., Epa, V. C., Garrett, T. P. & Ward, C. W. (2000). *Cell. Mol. Life Sci.* **57**, 1050–1093.
Breuhahn, K. & Schirmacher, P. (2008). *World J. Gastroenterol.* **14**, 1690–1698.
DeChiara, T. M., Efstratiadis, A. & Robertson, E. J. (1990). *Nature (London)*, **345**, 78–80.
Duguay, S. J., Jin, Y., Stein, J., Duguay, A. N., Gardner, P. & Steiner, D. F. (1998). *J. Biol. Chem.* **273**, 18443–18451.
Frasca, F., Pandini, G., Scalia, P., Sciacca, L., Mineo, R., Costantino, A., Goldfine, I. D., Belfiore, A. & Vigneri, R. (1999). *Mol. Cell. Biol.* **19**, 3278–3288.
Hizuka, N., Fukuda, I., Takano, K., Asakawa-Yasumoto, K., Okubo, Y. & Demura, H. (1998). *J. Clin. Endocrinol. Metab.* **83**, 2875–2877.
Hoet, R. M. *et al.* (2005). *Nature Biotechnol.* **23**, 344–348.
Jacobs, C. I. (2008). *Clin. Oncol.* **20**, 345–352.
Khosla, S., Ballard, F. J. & Conover, C. A. (2002). *J. Clin. Endocrinol. Metab.* **87**, 3867–3870.
Leighton, P. A., Ingram, R. S., Eggenschwiler, J., Efstratiadis, A. & Tilghman, S. M. (1995). *Nature (London)*, **375**, 34–39.
Leslie, A. G. W. (1992). *Jnt CCP4/ESF–EACBM Newsl. Protein Crystallogr.* **26**.
Newman, J. (2004). *Acta Cryst.* D**60**, 610–612.
Newman, J. (2005). *Acta Cryst.* D**61**, 490–493.
Newman, J., Egan, D., Walter, T. S., Meged, R., Berry, I., Ben Jelloul, M., Sussman, J. L., Stuart, D. I. & Perrakis, A. (2005). *Acta Cryst.* D**61**, 1426–1431.
Segelke, B. & Rupp, B. (1998). *Am. Crystallogr. Assoc. Meet. Ser.* **25**, 78.
Valenzano, K. J., Remmler, J. & Lobel, P. (1995). *J. Biol. Chem.* **270**, 16441–16448.